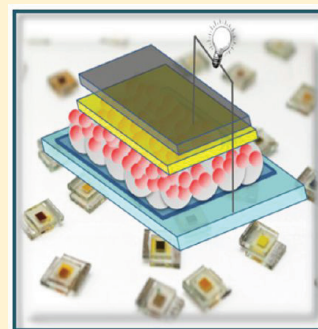


## Quantum Dot Solar Cells. *The Next Big Thing* in Photovoltaics

Prashant V. Kamat\*

Radiation Laboratory and Department of Chemistry and Biochemistry, University of Notre Dame, Notre Dame, Indiana 46556, United States

**ABSTRACT:** The recent surge in the utilization of semiconductor nanostructures for solar energy conversion has led to the development of high-efficiency solar cells. Some of these recent advances are in the areas of synthesis of new semiconductor materials and the ability to tune the electronic properties through size, shape, and composition and to assemble quantum dots as hybrid assemblies. In addition, processes such as hot electron injection, multiple exciton generation (MEG), plasmonic effects, and energy-transfer-coupled electron transfer are gaining momentum to overcome the efficiency limitations of energy capture and conversion. The recent advances as well as future prospects of quantum dot solar cells discussed in this perspective provide the basis for consideration as “*The Next Big Thing*” in photovoltaics.



Nanostructure architectures have facilitated the evolution of new strategies to design next-generation solar cells. Three major types of cells that have dominated research in recent years include (i) dye-sensitized solar cells (DSSC), (ii) bulk heterojunction (BHJ) photovoltaic cells or organic photovoltaic cells, and (iii) quantum dot solar cells (QDSC). The simplicity of the synthetic procedure, tunability of light absorption, sensitivity to diffused light, and ability to design flexible solar panels make semiconductor nanostructure an important candidate as a light absorber.<sup>1</sup> Figure 1 shows the principle of operation of three types of solar cells that employ semiconductor quantum dots (QDs) as photon harvesters.

The simplicity of the synthetic procedure, tunability of light absorption, sensitivity to diffused light, and ability to design flexible solar panels make the semiconductor nanostructure an important candidate as a light absorber.

The primary photochemical event in the case of DSSC is the injection of electrons from the excited dye into a mesoscopic semiconductor oxide, while in the case of BHJ solar cells, it is the excited interaction between the polymer and fullerene derivative and/or semiconductor QDs.<sup>3–5</sup> Manipulation of photoinduced charge separation in semiconductor QDs and their transport across the interface dictate the performance of QDSC.<sup>2</sup> Unlike single-crystal semiconductor photovoltaics, the transport of charge carriers in these cells is not field-driven but is kinetically driven.<sup>6,7</sup> The principle of the operation of nanostructured semiconductor-based solar cells was demonstrated more than two decades ago.<sup>8,9</sup> By transferring

photogenerated electrons quickly to an acceptor such as TiO<sub>2</sub> or by scavenging holes with a redox couple, it is possible to lengthen the lifetime of the charge carriers so that they can deliver photocurrent effectively. For example, ultrafast charge injection from excited dye into TiO<sub>2</sub> and quick scavenging of holes by the redox couple in QDSC, or regeneration of the dye in DSSC, facilitate accumulation of electrons within the mesoscopic TiO<sub>2</sub> films. By minimizing the recombination losses at the grain boundaries, the charge carriers are transported to the collecting electrode and thus deliver good power conversion efficiency for the corresponding solar cells.

The recent advances in BHJ and DSSC have been discussed in reviews and perspectives.<sup>3,6,10–15</sup> Efficiencies in the range of 12% for DSSC and 8% for BHJ solar cells have already been achieved.<sup>16,17</sup> The power conversion efficiency of liquid junction QDSC has increased from 1 to 5% during last couple of years. Efficiencies in the range of 7% have also been reported for solid-state QDSC.<sup>18,19</sup> A recent report of 10.9% efficiency for a perovskite-based solar cell has put QDSC on par with DSSC and BHJ solar cells.<sup>20</sup> The obvious question that one encounters is, *Will QDSC emerge as The Next Big Thing in Photovoltaics?* Recent approaches in utilizing semiconductor QDs for the design of QDSC and emerging strategies for the attainment of greater efficiency discussed here provide the basis for such an optimistic view.

*Designing Photoactive Nanostructured Semiconductor Electrodes.* The proper assembly and ordering of semiconductor QDs in a mesoscopic oxide film is an essential criterion for designing QDSC. The mesoscopic TiO<sub>2</sub> and ZnO films (5–10 μm thick) are cast on optically transparent electrodes (OTE). These electrodes are modified with QDs so that they serve as light

**Received:** January 8, 2013

**Accepted:** February 28, 2013

**Published:** February 28, 2013

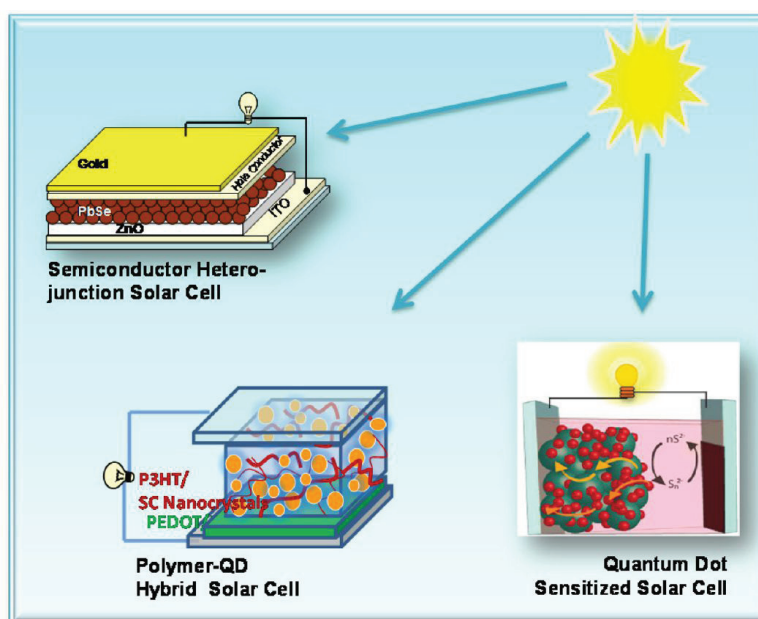


Figure 1. Schematic illustration of a semiconductor-nanostructure-based next-generation solar cells (Reproduced from ref 2).

The proper assembly and ordering of semiconductor QDs in a mesoscopic oxide film is an essential criterion for designing QDSC.

energy harvesters and convert incident photons to electricity. A brief description of various methods employed to cast semiconductor QD layers on mesoscopic  $\text{TiO}_2$  (or  $\text{ZnO}$  or  $\text{SnO}_2$ ) films is illustrated in Figure 2. A majority of the solid-state QDSC employ photoanodes prepared by the drop casting

or spin coating method. In this method, a known amount of the colloidal QD suspension is added onto the electrode surface, and the film is dried in a controlled way. The chemical bath deposition and surface ionic layer adsorption and reaction (SILAR) employ reactant precursors in solution that react on the electrode surface.<sup>21,22</sup> The growth of crystallites is controlled by the time of reaction or number of cycles of the SILAR process.

Electrophoretic deposition is carried out by applying a DC electric field between two electrodes immersed in a QD suspension.<sup>23,24</sup> A mixed polar/nonpolar solvent (e.g., toluene/ acetonitrile) allows negative charging of QD particles that are quickly driven to the positive electrode. The method allows

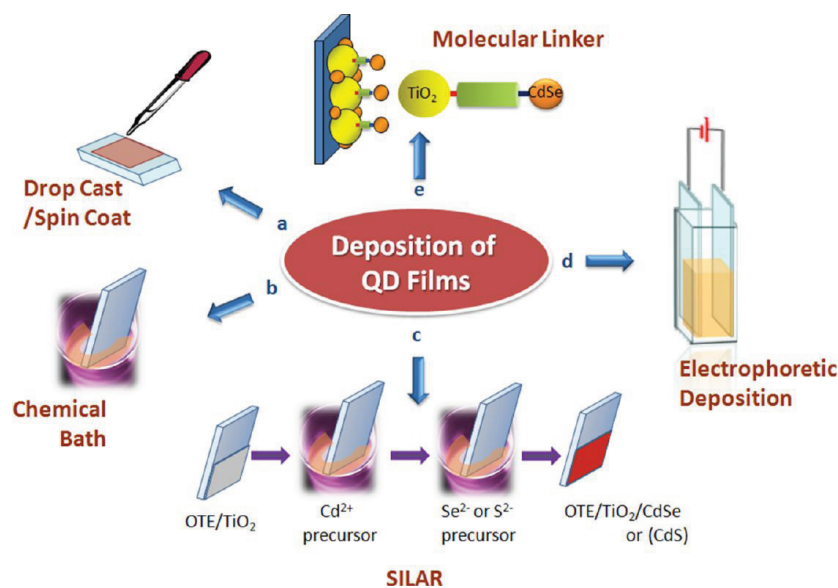
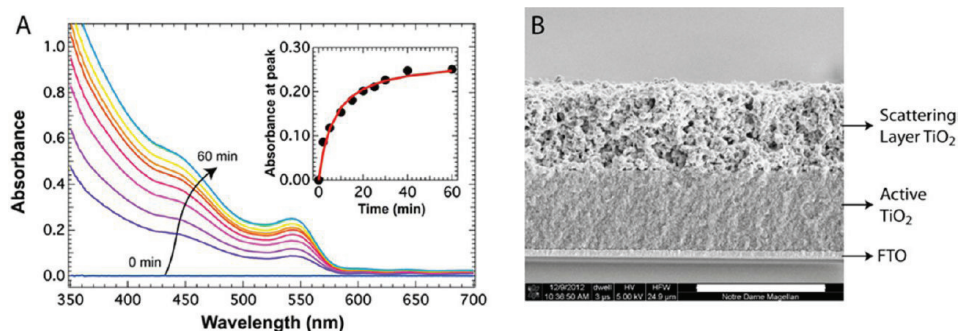


Figure 2. Schematic illustration of benchtop approaches of depositing a QD suspension on electrode surfaces. These methods include (a) drop casting or spin coating, (b) chemical bath deposition, (c) SILAR, (d) electrophoretic deposition, and (e) a bifunctional linker approach.



**Figure 3.** (A) Absorption spectra of a red QD attached to a transparent  $\text{TiO}_2$  by EPD with a bias voltage of 60 V at different times from 0 to 60 min. The data were collected at 0, 2, 5, 10, 15, 20, 25, 30, 40, and 60 min. The inset shows the variation of the absorption peak intensity at 550 nm with time. (B) Cross-sectional SEM image of the photoanode consisting of a  $\text{TiO}_2$  mesoscopic film loaded with QDs. The scale bar represents a length of 10  $\mu\text{m}$ . (Reproduced from ref 25.)

close packing of QD nanoparticles on a bare electrode or within the mesoscopic oxide ( $\text{TiO}_2$ ) film with no significant change in the particle size. By manipulating the concentration or time of deposition, it is possible to obtain the desired amount of QD loading on the electrode surface. Figure 3 shows an example of CdSeS QD deposition within the mesoscopic  $\text{TiO}_2$  film.<sup>25</sup>

Another popular method is the linker-assisted attachment of QD particles to the oxide surface.<sup>26,27</sup> This method allows selective attachment of presynthesized metal chalcogenide QDs (e.g., CdS, CdSe) to an oxide surfaces (e.g.,  $\text{TiO}_2$  or ZnO) using a bifunctional linker molecule such as 3-mercaptopropionic acid. The carboxylic acid group complexes with the  $\text{TiO}_2$  surface, while the thiol group interacts with QDs. This method allows submonolayer coverage with minimal aggregation of particles. The manipulation of linker length allows the study of distance-dependent interaction between  $\text{TiO}_2$  and CdSe nanoparticles. However, the linker molecule must be carefully selected because it can interact with the QD surface and modify surface defects.<sup>28,29</sup>

Each method discussed in this section has its own merit, and its choice depends upon the end goal or objective of the investigation. The room-temperature chemical bath and SILAR methods provide close contact between QDs and the oxide surface, and hence, these methods are excellent choices for preparing electrodes for solar cells. They are usually non-crystalline and may require annealing to introduce crystallinity. The advantage of electrophoretic deposition and linker-assisted deposition is the size selectivity of the QDs within the film. Because the hot injection synthesis allows size selectivity of crystalline QDs, it is easy to use these two latter methods for achieving QD deposition with tailored size and properties.

**Solar Cell Assembly and Performance Evaluation.** Two types of solar cell configurations currently dominate the recent research activities of QD photovoltaics, (i) solid-state semiconductor heterojunction solar cells (SHJSC) and (ii) liquid junction solar cells or QD-sensitized solar cells (QDSC). Both types of solar cells offer the convenience of benchtop fabrication with minimal necessity for a clean room or controlled atmosphere during solar cell assembly. This simple fabrication method alone provides the economic benefit toward the construction of a transformative photovoltaic technology. The schematic illustration shown in Figure 4 identifies different components of QDSC.

The majority of the published work on SHJSC has centered on lead chalcogenides.<sup>30,31</sup> Both PbS and PbSe QDs deposited on mesoscopic  $\text{TiO}_2$  or ZnO film serve as the photoanode.

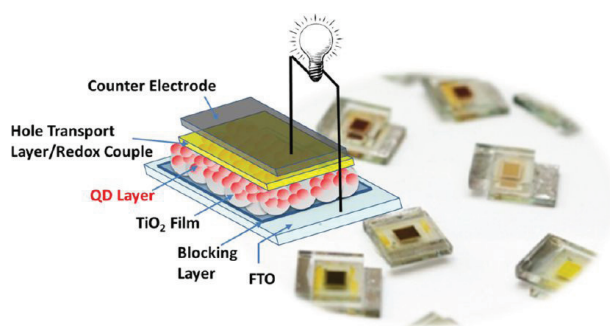


**Figure 4.** Anatomy of QDSC depicting different layers. The hole transport layer is a redox electrolyte in liquid junction solar cells and a solid-state hole-transporting layer in heterojunction solar cells. The background image shows a few QDSC samples prepared in our laboratory with an active QD layer ( $\sim 0.25 \text{ cm}^2$  area) sandwiched between the two OTE and the redox electrolyte.

Other semiconductors such as CdSe,  $\text{Sb}_2\text{S}_3$ , CIGS, and so forth have also been employed as photon harvesters. A hole scavenger such as CuSCN, PEDOT, or 2,2',7,7'-tetrakis(*N,N*-di-*p*-methoxyphenylamine)9,9'-spirobifluorene (spiro-OMeTAD) is then deposited onto these photoactive films. A thin layer of metal (e.g., Au or Ag) is deposited on top of the hole transport layer to make the electrical contact. Upon photoexcitation of the semiconductor QDs, the electrons are driven toward the oxide layer, and the holes are driven toward the metal contact and thus generate photocurrent. Through a series of iterative efforts, it has been possible to attain efficiencies as high as 7% for metal chalcogenide based solar cells.<sup>18</sup>

However, a new class of organometal halide perovskite based semiconductors has now emerged as the most viable candidate for QDSC surpassing the power conversion efficiencies rendered by the lead chalcogenide based BHJSC.<sup>19,20,32</sup> Methylammonium lead iodide chloride ( $\text{CH}_3\text{NH}_3\text{PbI}_2\text{Cl}$ ) perovskite is directly formed by first treating a mesoscopic oxide film with a precursor solution and then heating the film at 100  $^\circ\text{C}$ . The organometal halide formed on the oxide absorbs in the entire visible region (1.55 eV) and exhibits excellent external quantum efficiency. A power conversion efficiency of 10.9% has been reported under masked AM1.5 illumination (Figure 5).

The principle of operation of QDSC is based on the semiconductor–liquid junction photoelectrochemistry.<sup>33,34</sup>



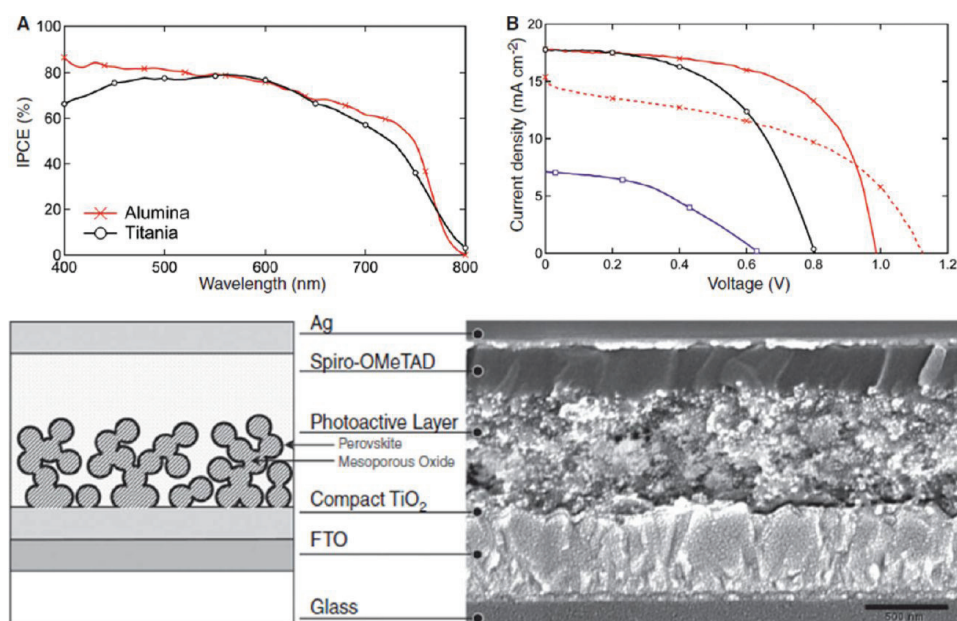


**Figure 5.** (A) IPCE action spectrum of an  $\text{Al}_2\text{O}_3$ -based and perovskite-sensitized  $\text{TiO}_2$  solid-state heterojunction solar cell, with the device structure as follows: FTO/compact  $\text{TiO}_2$ /mesoporous  $\text{Al}_2\text{O}_3$  (red trace with crosses) or mesoporous  $\text{TiO}_2$  (black trace with circles)/ $\text{CH}_3\text{NH}_3\text{PbI}_2\text{Cl}$ /spiro-OMeTAD/Ag. (B) Current density–voltage characteristics under simulated AM1.5  $100 \text{ mW cm}^{-2}$  illumination for  $\text{Al}_2\text{O}_3$ -based cells, one cell exhibiting high efficiency (red solid trace with crosses) and one exhibiting  $V_{\text{OC}} > 1.1 \text{ V}$  (red dashed line with crosses), for a perovskite-sensitized  $\text{TiO}_2$  solar cell (black trace with circles), and for a planar-junction diode with the structure FTO/compact  $\text{TiO}_2$ / $\text{CH}_3\text{NH}_3\text{PbI}_2\text{Cl}$ /spiro-OMeTAD/Ag (purple trace with squares). The bottom panel shows a schematic representation of the full device structure and a cross-sectional SEM image (scale bar, 500 nm). (From ref 20. Reprinted with permission of The American Association for the Advancement of Science.)

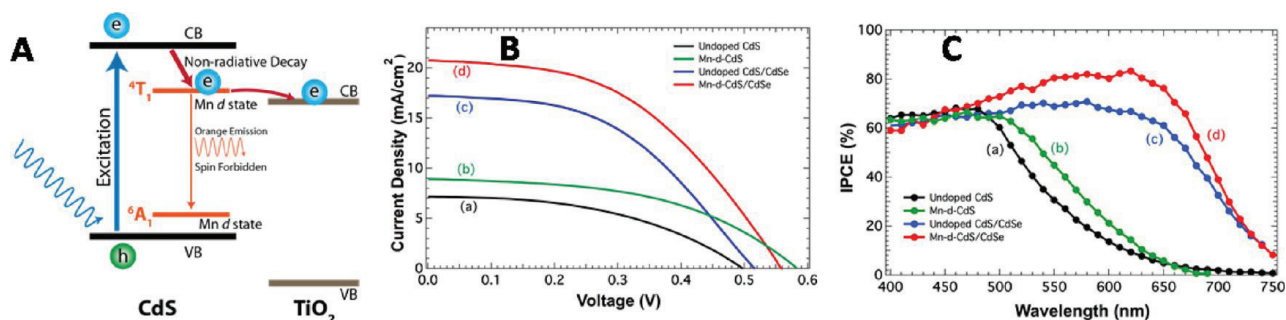


**Figure 6.** (A) Schematic representation of the energy diagram of Mn-doped CdS. The electron from the conduction band of CdS transfers to the Mn d state ( ${}^4\text{T}_1$ ) within a few picoseconds, but the Mn d–d transition has a lifetime in the range of several hundreds of microseconds due to the spin and orbitally forbidden transition.<sup>39</sup> (B)  $J$ – $V$  characteristics and (C) Incident photon to charge carrier generation efficiency (IPCE) response of different working electrodes measured under simulated AM 1.5 sunlight ( $100 \text{ mW/cm}^2$ ). (a) Undoped CdS, (b) Mn-doped CdS, (c) undoped CdS/CdSe, and (d) Mn-doped CdS/CdSe. The working electrode areas were 0.20, 0.20, 0.22, and 0.22  $\text{cm}^2$ , respectively (with a  $\text{Cu}_2\text{S/RGO}$  counter electrode and aqueous  $1 \text{ M S}^{2-}/1 \text{ M S}$  as the electrolyte). (Reproduced from ref 40.)

Most of the QDSSC fabrication reported to date employs CdSe and CdS semiconductor QDs that are deposited on mesoscopic oxide films. The sulfide/polysulfide electrolyte acts as a hole transporter. The casting of a blocking layer on the FTO surface (10–20 nm thick layer of close packed  $\text{TiO}_2$ ) before the deposition of mesoscopic  $\text{TiO}_2$  films is important to achieve higher photovoltage as it blocks the contact of the FTO surface with the redox electrolyte.  $\text{Cu}_2\text{S}$ -based counter electrodes that exhibit redox activity toward the  $\text{S}^{2-}/\text{S}_n^{2-}$  couple deliver higher fill factors and steady photocurrent with good photostability.<sup>35</sup> In recent years, two or more semiconductor QDs have been coupled to achieve improved charge separation.<sup>36,37</sup> Often, a ZnS blocking layer on CdSe is deposited to suppress back electron transfer to the redox couple.<sup>38</sup>

Electronic and photophysical properties of QDs can be tuned by doping to the optically active transition metal ions (e.g.,  $\text{Mn}^{2+}$ ).<sup>41–45</sup> The dopant creates electronic states in the midgap region of the QD, thus altering the charge separation and recombination dynamics. Synthesis of Mn-doped II–VI semiconductor QDs has been reported earlier.<sup>46–48</sup> Because the Mn d–d transition ( ${}^4\text{T}_1$ – ${}^6\text{A}_1$ ) is both spin and orbitally forbidden, we observe a relatively long lifetime of the excited state.<sup>44,49,50</sup> The midgap states created by Mn doping trap electrons and screen them from charge recombination with holes and/or the oxidized polysulfide electrolyte. By using this doping strategy, we have succeeded in achieving an efficiency of 5.4% for QDSC with Mn-doped CdS/CdSe as the photoanode under AM 1.5 solar illumination (Figure 6). More details on

this strategy can be found elsewhere.<sup>40</sup> Additionally, attention is now being drawn to the utilization of ternary metal chalcogenide semiconductors (for example, CdSeS and CuInS<sub>2</sub>) in solar cells.<sup>51–54</sup> These semiconductor QDs allow tuning of photophysical properties as well as band gap engineering by varying the composition of the metal cation or chalcogenide anion.

Whereas quick transfer of electrons to the oxide layer and holes to an acceptor (hole transport layer) or redox couple are the primary events that dictate the photon conversion efficiency, loss of electrons through interfacial recombination processes and discharge of electrons at the counter electrode determine the overall power conversion efficiency.

*Interfacial Charge-Transfer Processes Dictating the QDSC Performance.* One of the key factors in the continuous operation of QDSC is the efficient transport of charge carriers (electrons and holes) toward the opposing electrodes. Whereas quick transfer of electrons to the oxide layer and holes to an acceptor (hole transport layer) or redox couple are the primary events that dictate the photon conversion efficiency, loss of electrons through interfacial recombination processes and discharge of electrons at the counter electrode determine the overall power conversion efficiency. Figure 7 shows some key reaction steps

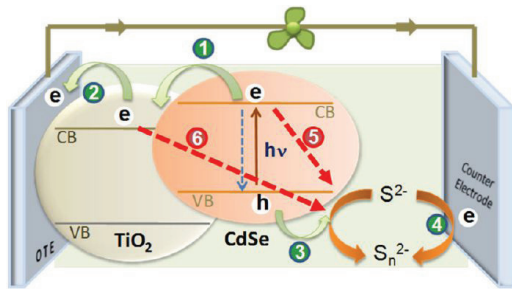


**Figure 7.** Schematic illustration of photoinduced charge-transfer processes following a laser pulse excitation: (1) Charge injection from excited CdSe into TiO<sub>2</sub>; (2) transport of electrons to the collecting electrode surface; (3) hole transfer to the redox couple; (4) regeneration of the redox couple; (5) recombination of electrons from CdSe and the oxidized form of the redox couple; and (6) interfacial recombination of electrons from TiO<sub>2</sub> and the oxidized form of the redox couple. (Reproduced from ref 2.)

that dictate the overall efficiency of a CdSe-based liquid junction QDSC employing S<sup>2-</sup>/S<sub>n</sub><sup>2-</sup> as the redox couple. Details on the charge-transfer kinetics can be found in an earlier review.<sup>2</sup> The initial electron transfer between CdSe and TiO<sub>2</sub> is an ultrafast process and occurs with a rate constant of the order of 10<sup>10</sup>–10<sup>11</sup> s<sup>-1</sup>.<sup>55</sup> However, the limiting factor in the overall charge-transfer kinetics is the slow hole transfer, which occurs with a rate constant that is 2–3 orders of magnitude less than

that of the electron injection.<sup>56</sup> The electron transport and charge recombination processes have been studied by impedance spectroscopy.<sup>7</sup> Because of the slower electron transport within the mesoscopic TiO<sub>2</sub> film, the recombination losses become a major factor in limiting the overall efficiency.

*Emerging Strategies to Boost the Solar Cell Performance.* Several new approaches have emerged to boost the efficiency of QDSC in recent years. The emergence of new approaches will not only provide ways to increase the photoconversion efficiency, but they will also pave the way toward a fundamental understanding of new phenomena related to excited-state dynamics at various interfaces of hybrid assemblies. A few selected themes that hold promise are discussed here.

(a) Multiple Exciton Generation (MEG) and Hot Electron Transfer. Utilization of high-energy photons to generate multiple charge carriers<sup>30,58–63</sup> or capturing hot electrons<sup>60,64–66</sup> before their thermalization can boost the operation efficiency of QDSC. Figure 8 shows the principle of MEG in semiconductor QDs and the boost in power conversion efficiency that one can expect for different band gap semiconductors with a varying MEG threshold for photon energy.<sup>57</sup> Spectroscopic measurements carried out with lead chalcogenides have shown that these charge carriers are short-lived and their capture to produce photocurrent in a solar cell remains a challenge.<sup>58,59</sup> Recent studies, however, have proven the feasibility of this concept, with demonstration of an external quantum efficiency greater than 100% at wavelengths below 400 nm.<sup>67</sup> Further concerted efforts are necessary to design semiconductor QD hybrid systems that can deliver MEG and hot electrons and incorporate them as building blocks in light energy conversion devices.

(b) Plasmonic Solar Cells (Exploring Exciton–Plasmon Interactions). The plasmon resonances of silver and gold nanoparticles have been widely explored in DSSC, BHJ solar cells, and photocatalysis.<sup>69–74</sup> By coupling semiconductor nanostructures with metal nanoparticles, it is possible to improve the photocatalytic or photovoltaic conversion efficiency. A major argument for the observed improvement in photoconversion efficiency is put forth on the basis of localized surface plasmon (SP) resonance near the photoactive molecules and/or near the semiconductor particle, which induces better charge separation. Other explanations include (i) increased absorption due to SPs and light trapping effects,<sup>75</sup> (ii) creation of a localized electric field, (iii) direct participation of electron transfer from metal nanoparticles, and (iv) electron storage effects that can drive the Fermi level to more negative potentials. Although semiconductor–metal nanocomposites have been widely used in photocatalysis (e.g., water splitting reactions), surprisingly few studies exist that explore plasmonic effect in QDSC. It is interesting to note that SP resonance coupled with electron charging effects play an important role in the manifestation of semiconductor–metal devices.<sup>76</sup> In addition, if the semiconductor (e.g., CdSe) is quantized, the strong coupling between the lowest excited state or excitonic transition and SP of the neighboring metal surface needs to be taken into account.<sup>68,77</sup> A schematic representation of SP coupling with the excited semiconductor QDs is shown in Figure 9. A few studies in recent years have focused on studying the influence of neighboring plasmonic (Au) nanoparticles on the excited dynamics of luminescent semiconductor QDs.<sup>78,79</sup> For example, the photoluminescent behavior of individual CdSe nanocrystals attached to silica-coated Au nanoparticles shows a separation-distance-dependent enhanced photoluminescence

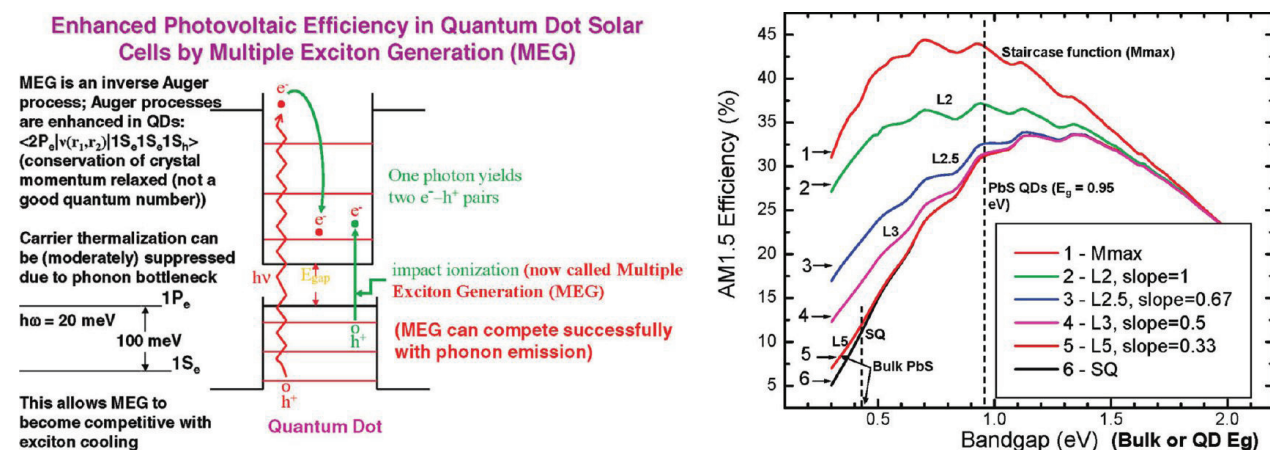


**Figure 8.** (Left panel) Schematic diagram illustrating the principle of MEG (multiple exciton generation) in QDs. (Right panel) Shockley and Queisser Limit calculations for PV power conversion efficiency for various MEG characteristics in QD solar cells compared to PV cells based on bulk semiconductors.  $L(n)$  represents the MEG photon energy threshold in units of the number of band gaps of energy, and the slope value is the MEG efficiency (extra excitons/band gap of the photon energy) beyond the MEG threshold. (Reproduced from ref 57.)

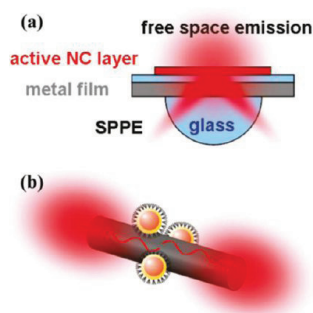


**Figure 9.** Typical configurations of metal–semiconductor nanostructures that lead to exciton–SP energy transfer. (a) Excited semiconductor NCs that are deposited on a metal film release their energy into free space emission or excite SPs on the metal surface that then can decay radiatively and generate SP emission (SPPE). A dielectric spacer layer prevents close contact between metal and semiconductor components and avoids NC emission quenching caused by coupling to lossy surface waves. (b) NCs attached to a metal nanorod can excite single SPs that propagate along the metal wire, enabling nanoscale energy transport and localization. Because the propagating SPs rapidly remove the energy from the location of the NCs, energy back transfer is unlikely. (Reproduced from ref 68.)

intensity, suppressed off-states, as well as shorter lifetimes in comparison with those of the isolated CdSe nanocrystals.<sup>78</sup> While several studies report enhanced efficiency in plasmonic solar cells,<sup>80–82</sup> effective use of exciton–plasmon interactions in QDSC is yet to be realized fully, and this area of research offers opportunities to develop new strategies for QD photovoltaics. The emergence of new approaches will not only provide ways to increase the photoconversion efficiency, but they will also pave the way toward a fundamental understanding of new phenomena related to excited-state dynamics at various interfaces of hybrid assemblies.

(c) **Supersensitization of QDs with Dye Molecules.** A good spectral match between sensitizer absorption and incident solar radiation is an important criterion in designing light energy conversion systems. Semiconductors such as CdS and CdSe absorb only in the visible. With size quantization effects, their absorption edge is further driven to lower-wavelength regions.

The emergence of new approaches will not only provide ways to increase the photoconversion efficiency, but they will also pave the way toward a fundamental understanding of new phenomena related to excited-state dynamics at various interfaces of hybrid assemblies.

One approach to maximize the absorption range of incident photons is to couple the short band gap semiconductor with dye molecules.<sup>83–87</sup> Integrating semiconductor QDs and the dye components in a suitable manner can be effective in enhancing the photocurrent generation in QDSC. Two different approaches are indicated in Figure 10.

In the first example, both QDs and dye molecules upon excitation participate separately in the charge injection process. Supersensitization of QDs (e.g., CdS) with a sensitizing dye absorbing in the red region was recently reported by Zaban and co-workers.<sup>87,88</sup> CdS QD–TiO<sub>2</sub>–dye (N719) bilayer cosensitization facilitated the use of the  $I^-/I_3^-$  couple. A similar concept was used to anchor a CdS QD that absorbs in the visible region on a mesoscopic TiO<sub>2</sub> film followed by capping of a thin Al<sub>2</sub>O<sub>3</sub> layer.<sup>86</sup> A squaraine dye was also attached to this hybrid structure to capture photons in the NIR region (Figure 10A). The squaraine dye employed in this study was energetically capable of regenerating CdS by capturing photogenerated holes while concurrently serving as a sensitizer in the red–IR region. This dual role of squaraine dye was achieved by the inclusion of a thin Al<sub>2</sub>O<sub>3</sub> barrier layer between CdS and the adsorbed dye layer.

In the second example, the QDs and the dye molecules operate in a synergistic manner. For example, sequentially assembled CdSe QDs and squaraine dye (SQSH) on a mesoscopic TiO<sub>2</sub> film enables coupling of energy- and electron-transfer processes to generate photocurrent in a hybrid solar cell (Figure 10B).<sup>89</sup> When attached separately, both CdSe



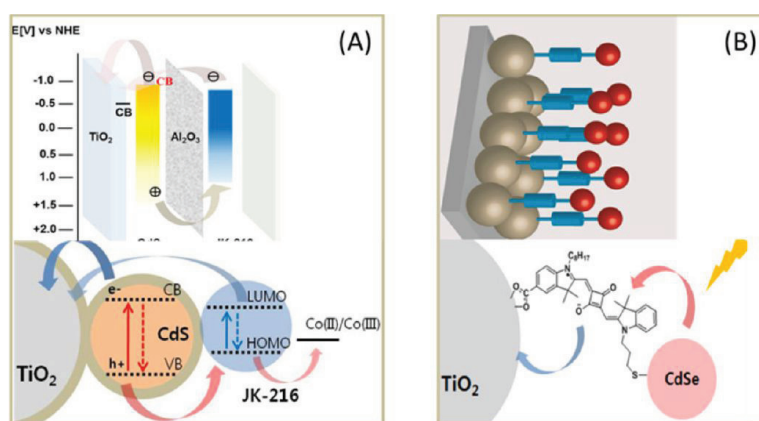


**Figure 10.** (A) Supersensitization of a nanocrystalline  $\text{TiO}_2$  film with CdSe and squaraine dye (blue arrow: electron transfer; red arrow: hole transfer). (B) Energy- and electron-transfer processes in a  $\text{TiO}_2$ /SQSH/CdSe hybrid assembly (red arrow: energy transfer from excited CdSe to SQSH; blue arrow: electron transfer from excited SQSH into  $\text{TiO}_2$ ). (Reproduced from refs 86 and 89.)

QDs and SQSH are capable of injecting electrons into  $\text{TiO}_2$  under visible and near-IR irradiation, respectively. If CdSe QDs are linked to SQSH dye, we observe energy transfer from excited CdSe (3.7 nm diameter QD) into SQSH as the emission of the QD and the absorption of the dye overlap. The Förster resonance energy transfer (FRET) between excited CdSe and the dye molecule allows effective utilization of visible photons by transfer as energy to the red–near-IR absorbing SQSH. Thus, SQSH can be excited by direct excitation in the red–near-IR region and via FRET in the visible region (Figure 10B). The ability to capture energy from excited CdSe via FRET and inject electrons into  $\text{TiO}_2$  was realized from the broader response of the solar cell.<sup>89</sup> The hybrid solar cells prepared with SQSH as a linker between CdSe and  $\text{TiO}_2$  exhibited a power conversion efficiency of 3.65%, which is greater than the efficiency observed with CdSe (0.15%) or SQSH (3.15%) alone. Coupling FRET and electron transfer in a synchronized manner is another unexplored area of solar cell research. It provides a convenient strategy to mimic photosynthesis by harvesting photons from selective regions of the solar spectrum and to couple energy and electron-transfer processes in a synergistic manner.

(d) Tandem Layered QDSC. Because size quantization offers the ability to tune the absorption properties of semiconductor QDs, it should be possible to assemble two (or more) different QDs in an ordered fashion to increase the absorption in the visible region. Several recent studies have employed sequential or codeposition of CdSe and CdS QDs on  $\text{TiO}_2$  films to improve photoelectrochemical performance.<sup>35,90–92</sup> One of the possibilities to engineer the light-harvesting features over a broader region and utilize the photons more effectively is to develop a tandem structure of semiconductor QDs such that the absorption of photons within the film is carried out in a systematic and gradient fashion (Figure 11A and B).

In a recent study, we reported synthesis of highly luminescent 4.5 nm CdSeS QDs with a gradient structure that allows tuning of absorption and emission bands in the entire visible region without varying the particle size.<sup>25</sup> The electrophoretic deposition of these QDs enabled us to design tandem layers of CdSeS of varying the band gap within the mesoscopic  $\text{TiO}_2$  film. The photoactive anode exhibited an increased power conversion efficiency of 3.2–3.0% in two- and

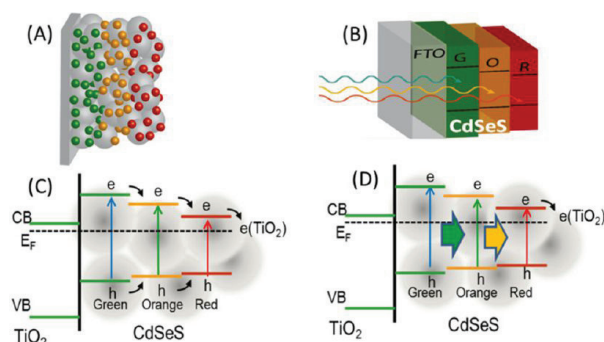


**Figure 11.** (A,B) Deposition of CdSeS QDs in a tandem fashion. Illustration of (C) electron-transfer and (D) energy-transfer processes between the green/orange/red QD assembled in a tandem architecture. The electrons are injected from the red QD into  $\text{TiO}_2$ . (Reproduced from ref 25.)

three-layered tandem QDSC as compared to 1.97–2.81% with single-layered CdSeS.

Figure 11C and D illustrates two possible mechanisms with which we can observe the synergy of tandem layered QDs. In the first case, the alignment of band energies allows an electron-transfer cascade from larger-band-gap QDs to smaller-band-gap QDs, thus facilitating the accumulation of electrons in the latter. These electrons are then injected into  $\text{TiO}_2$  nanoparticles and transported across the  $\text{TiO}_2$  network. The other scenario involves energy transfer from larger-band-gap QDs to smaller-band-gap QDs, thus concentrating excitation in the red QDs. In this system, red QDs are the major participants in the electron-transfer process. Spectroscopic measurements in the future can resolve the contribution of these two processes and their effectiveness in improving the efficiency of photon capture and conversion to electricity.

(e) Nanowire–QD Composites. There have been several studies to sensitize ZnO nanowires (NWs) or nanorods with metal chalcogenide QDs.<sup>93–95</sup> Recent breakthrough in achieving 13.8% photoconversion efficiency with millimeter-sized arrays of p–i–n-doped InP nanowires has brought renewed interest in nanowire-based solar cells.<sup>96</sup> Alternatively, one can also employ metal chalcogenide NWs to construct solar cells. One of the advantages of using CdSe nanowires for the solar cell application is that these NWs can act as both the

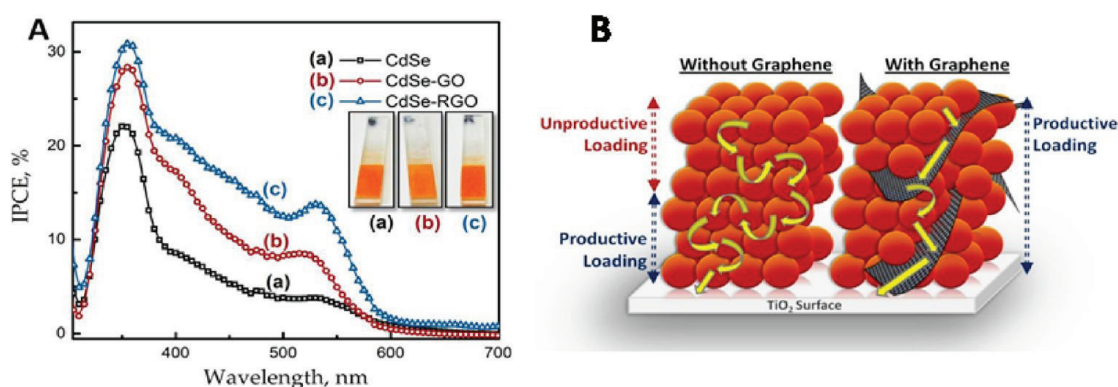


**Figure 12.** (A) IPCE of CdSe and CdSe–RGO composite films cast on OTE. The contribution of CdSe QDs ( $\sim 530$  nm) to the overall current generation is markedly improved in CdSe–RGO films. (B) Schematic illustration comparing the electron transport in CdSe and CdSe–RGO composites. (Reproduced from ref 100.)

sensitizer and carrier transport scaffold. Such a network of NWs can minimize the recombination losses during charge transport that is commonly experienced in the interconnected network of mesoscopic semiconductor films.<sup>97,98</sup> The use of a semiconductor NW/QD composite in solar cells is relatively less studied. Incorporating colloidal CdSe QDs within the nanowire architecture has recently been shown to increase the power conversion efficiencies by a factor of 2.<sup>99</sup> The synergy of employing NW/QD composites can be realized from the fact that the overall external quantum efficiency increases across the entire visible spectrum, even at wavelengths where the QDs do not absorb light. The ability to achieve better charge separation and increase the overall absorptive range in a semiconductor NW/QD composite offers new opportunities to develop solar cells.

(f) Semiconductor–Carbon Nanomaterial Hybrids. Incorporation of carbon nanomaterials such as single-wall carbon nanotubes (SWCNT) or reduced graphene oxide (RGO) in mesoscopic QD films offers a significant advance toward overcoming conductivity problems inherent to QD films.<sup>101</sup> The role of SWCNT and RGO as conduits to capture and transport electrons in the mesoscopic semiconductor films has been demonstrated by casting mesoscopic  $\text{TiO}_2$  films containing SWCNT or RGO. Their ability to improve charge separation in semiconductor systems is well-established.<sup>102,103</sup> The composites of graphene oxide (or carbon nanotubes or nanocups) can be electrophoretically deposited onto a conducting glass electrode and then assembled in solar cells.<sup>102,103</sup>

Figure 12, which shows an example of the IPCE of CdSe–RGO films, highlights the important role that graphene plays in mediating electron transfer from CdSe QDs to the current-collecting electrode (Figure 12A).<sup>100</sup> The IPCE contribution from the CdSe absorption peak at 530 nm increases from 3.8% in CdSe-only films to 13.8% in CdSe–RGO composites. By introducing graphene oxide, photogenerated electrons in CdSe QD layers farthest from the  $\text{TiO}_2$  network can be transported toward the collecting electrode surface.

**Future Outlook.** The desire to develop a competitive photovoltaic technology has brought great enthusiasm among chemists, physicists, material scientists, and engineers. Many new and interesting scientific advances have been made in recent years along with significant strides in attaining higher power conversion efficiency. Among the next-generation solar cells, DSSC and organic photovoltaics have dominated the

research efforts during the last 2 decades. QDSC, however, are emerging as serious contenders to these two nearly matured technologies. All three types of solar cells operate on the simple principle of photoinduced electron transfer and interfacial charge separation.

In the cases of DSSC and BHJ solar cells, the maximum attainable efficiency seems to be approaching the thermodynamic limit. The maximum power conversion efficiency of 10–12% reported in the literature often deals with small area electrodes. A significant decrease in efficiency ( $\sim 25\%$ ) can be anticipated if these solar cells are to be transformed into larger solar panels. The recent perspective by Peter<sup>15</sup> discusses the future challenges in DSSC research and limitations of achieving further leaps in power conversion efficiency. Despite the initial success in demonstrating practically viable solar cells for niche applications, these technologies are yet to take a foothold in the broader solar cell market. The market competition, photostability issues, and economic factors will determine the viability of these technologies in the future.

To make a major impact in photovoltaics, it is necessary to implement a transformative technology. The advances in nanoscience and QDSC development offer new opportunities to make such a difference.

To make a major impact in photovoltaics, it is necessary to implement a transformative technology. The advances in nanoscience and QDSC development offer new opportunities to make such a difference. For example, recent efforts to develop a solar paint with semiconductor nanocrystals highlights the concept of a viable transformative approach.<sup>104</sup> Other approaches such as solar ink printing and reel-to-reel flexible photovoltaics also offer similar opportunities.<sup>105</sup> First Solar, a U.S. based company, has already made a stride in marketing economically viable CdTe/CdS thin-film-based solar panels worldwide. Several interesting factors laid down in this Perspective highlight salient features of QDSC and new strategies that can put this technology at the helm of next-generation solar cells. The recent success with perovskite-based



solar cells further ascertains the basis for an optimistic view of making QDSC the *Next Big Thing* in photovoltaics.

## AUTHOR INFORMATION

### Corresponding Author

\*E-mail: pkamat@nd.edu.

### Notes

The authors declare no competing financial interest.

### Biography

Prashant V. Kamat is a John A. Zahm Professor of Science in the Department of Chemistry and Biochemistry and the Radiation Laboratory and a Concurrent Professor in the Department of Chemical and Biomolecular Engineering, University of Notre Dame. His major research interests are in the areas of photoinduced charge-transfer processes in semiconductor nanocrystal-based architectures, photocatalytic aspects of metal nanoparticles and carbon nanostructures, and designing light-harvesting assemblies for next-generation solar cells. See <http://www.nd.edu/~pkamat> for further details.

## ACKNOWLEDGMENTS

The research described herein was supported by the Office of Basic Energy Sciences of the U.S. Department of Energy (DE-FC02-04ER15533). This is contribution NDRL 4954 from the Notre Dame Radiation Laboratory. I would like to thank the present and past researchers of the group who have actively contributed to QD solar cell research at Notre Dame. The results discussed in the Perspective have been extracted from references, and corresponding contributions of individual researchers is acknowledged.

## REFERENCES

- (1) Kamat, P. V.; Tvrđy, K.; Baker, D. R.; Radich, J. G. Beyond Photovoltaics: Semiconductor Nanoarchitectures for Liquid Junction Solar Cells. *Chem. Rev.* **2010**, *110*, 6664–6688.
- (2) Kamat, P. V. Boosting the Efficiency of Quantum Dot Sensitized Solar Cells Through Modulation of Interfacial Charge Transfer. *Acc. Chem. Res.* **2012**, *45*, 1906–1915.
- (3) Hagfeldt, A.; Boschloo, G.; Sun, L.; Kloo, L.; Pettersson, H. Dye-Sensitized Solar Cells. *Chem. Rev.* **2010**, *110*, 6595–6663.
- (4) Miyasaka, T. Toward Printable Sensitized Mesoscopic Solar Cells: Light-Harvesting Management with Thin TiO<sub>2</sub> Films. *J. Phys. Chem. Lett.* **2011**, *2*, 262–269.
- (5) Chang, J. A.; Rhee, J. H.; Im, S. H.; Lee, Y. H.; Kim, H.-J.; Seok, S. I.; Nazeeruddin, M. K.; Gratzel, M. High-Performance Nanostructured Inorganic–Organic Heterojunction Solar Cells. *Nano Lett.* **2010**, *10*, 2609–2612.
- (6) Bisquert, J.; Garcia-Belmonte, G. On Voltage, Photovoltage, and Photocurrent in Bulk Heterojunction Organic Solar Cells. *J. Phys. Chem. Lett.* **2011**, *2*, 1950–1964.
- (7) Hod, I.; Gonzalez-Pedro, V.; Tachan, Z.; Fabregat-Santiago, F.; Ivan, M.-S.; Bisquert, J.; Zaban, A. Dye versus Quantum Dots in Sensitized Solar Cells: Participation of Quantum Dot Absorber in the Recombination Process. *J. Phys. Chem. Lett.* **2011**, *2*, 3032–3035.
- (8) Gerischer, H.; Luebke, M. A Particle Size Effect in the Sensitization of TiO<sub>2</sub> Electrodes by a CdS Deposit. *J. Electroanal. Chem.* **1986**, *204*, 225–7.
- (9) Hodes, G.; Howell, I. D. J.; Peter, L. M. Nanocrystalline Photoelectrochemical Cells. A New Concept in Photovoltaic Cells. *J. Electrochem. Soc.* **1992**, *139*, 3136–40.
- (10) Li, C.; Liu, M.; Pschirer, N. G.; Baumgarten, M.; Mullen, K. Polyphenylene-Based Materials for Organic Photovoltaics. *Chem. Rev.* **2010**, *110*, 6817–6855.
- (11) Clarke, T. M.; Durrant, J. R. Charge Photogeneration in Organic Solar Cells. *Chem. Rev.* **2010**, *110*, 6736–6767.
- (12) Hains, A. W.; Liang, Z.; Woodhouse, M. A.; Gregg, B. A. Molecular Semiconductors in Organic Photovoltaic Cells. *Chem. Rev.* **2010**, *110*, 6689–6735.
- (13) Chu, T. Y.; Lu, J. P.; Beaupre, S.; Zhang, Y. G.; Pouliot, J. R.; Wakim, S.; Zhou, J. Y.; Leclerc, M.; Li, Z.; Ding, J. F.; et al. Bulk Heterojunction Solar Cells Using Thieno[3,4-c]pyrrole-4,6-dione and Dithieno[3,2-b:2',3'-d]silole Copolymer with a Power Conversion Efficiency of 7.3%. *J. Am. Chem. Soc.* **2011**, *133*, 4250–4253.
- (14) Zidek, K.; Zheng, K. B.; Ponseca, C. S.; Messing, M. E.; Wallenberg, L. R.; Chabera, P.; Abdellah, M.; Sundstrom, V.; Pullerits, T. Electron Transfer in Quantum-Dot-Sensitized ZnO Nanowires: Ultrafast Time-Resolved Absorption and Terahertz Study. *J. Am. Chem. Soc.* **2012**, *134*, 12110–12117.
- (15) Peter, L. M. The Gratzel Cell: Where Next? *J. Phys. Chem. Lett.* **2011**, *2*, 1861–1867.
- (16) Yella, A.; Lee, H. W.; Tsao, H. N.; Yi, C. Y.; Chandiran, A. K.; Nazeeruddin, M. K.; Diau, E. W. G.; Yeh, C. Y.; Zakeeruddin, S. M.; Gratzel, M. Porphyrin-Sensitized Solar Cells with Cobalt (II/III)-Based Redox Electrolyte Exceed 12% Efficiency. *Science* **2011**, *334*, 629–634.
- (17) He, F.; Yu, L. How Far Can Polymer Solar Cells Go? In Need of a Synergistic Approach. *J. Phys. Chem. Lett.* **2011**, *2*, 3102–3113.
- (18) Ip, A. H.; Thon, S. M.; Hoogland, S.; Voznyy, O.; Zhitomirsky, D.; Debnath, R.; Levina, L.; Rollny, L. R.; Carey, G. H.; Fischer, A.; et al. Hybrid Passivated Colloidal Quantum Dot Solids. *Nat. Nanotechnol.* **2012**, *7*, 577–582.
- (19) Kim, H. S.; Lee, C. R.; Im, J. H.; Lee, K. B.; Moehl, T.; Marchioro, A.; Moon, S. J.; Humphry-Baker, R.; Yum, J. H.; Moser, J. E. Lead Iodide Perovskite Sensitized All-Solid-State Submicron Thin Film Mesoscopic Solar Cell with Efficiency Exceeding 9%. *Sci. Rep.* **2012**, *2*, 591.
- (20) Lee, M. M.; Teuscher, J.; Miyasaka, T.; Murakami, T. N.; Snaith, H. J. Efficient Hybrid Solar Cells Based on Meso-Structured Organometal Halide Perovskites. *Science* **2012**, *338*, 643–647.
- (21) Switzer, J. A.; Hodes, G. Electrodeposition and Chemical Bath Deposition of Functional Nanomaterials. *MRS Bull.* **2010**, *35*, 743–752.
- (22) Baker, D. R.; Kamat, P. V. Photosensitization of TiO<sub>2</sub> Nanostructures with CdS Quantum Dots. Particulate versus Tubular Support Architectures. *Adv. Funct. Mater.* **2009**, *19*, 805–811.
- (23) Islam, M. A.; Herman, I. P. Electrodeposition of Patterned CdSe Nanocrystal Films Using Thermally Charged Nanocrystals. *Appl. Phys. Lett.* **2002**, *80*, 3823–3825.
- (24) Brown, P.; Kamat, P. V. Quantum Dot Solar Cells. Electrophoretic Deposition of CdSe–C<sub>60</sub> Composite Films and Capture of Photogenerated Electrons with nC<sub>60</sub> Cluster Shell. *J. Am. Chem. Soc.* **2008**, *130*, 8890.
- (25) Santra, P.; Kamat, P. V. Tandem Layered Quantum Dot Solar Cells. Tuning the Photovoltaic Response with Luminescent Ternary Cadmium Chalcogenides. *J. Am. Chem. Soc.* **2013**, *135*, 877–885.
- (26) Robel, I.; Subramanian, V.; Kuno, M.; Kamat, P. V. Quantum Dot Solar Cells. Harvesting Light Energy with CdSe Nanocrystals Molecularly Linked to Mesoscopic TiO<sub>2</sub> Films. *J. Am. Chem. Soc.* **2006**, *128*, 2385–2393.
- (27) Watson, D. F. Linker-Assisted Assembly and Interfacial Electron-Transfer Reactivity of Quantum Dot Substrate Architectures. *J. Phys. Chem. Lett.* **2010**, *1*, 2299–2309.
- (28) Baker, D. R.; Kamat, P. V. Tuning the Emission of CdSe Quantum Dots by Controlled Trap Enhancement. *Langmuir* **2010**, *26*, 11272–11276.
- (29) Tagliazucchi, M.; Tice, D. B.; Sweeney, C. M.; Morris-Cohen, A. J.; Weiss, E. A. Ligand-Controlled Rates of Photoinduced Electron Transfer in Hybrid CdSe Nanocrystal/Poly(viologen) Films. *ACS Nano* **2011**, *5*, 9907–9917.
- (30) Nozik, A. J.; Beard, M. C.; Luther, J. M.; Law, M.; Ellingson, R. J.; Johnson, J. C. Semiconductor Quantum Dots and Quantum Dot Arrays and Applications of Multiple Exciton Generation to Third-Generation Photovoltaic Solar Cells. *Chem. Rev.* **2010**, *110*, 6873–6890.

- (31) Kramer, I. J.; Sargent, E. H. Colloidal Quantum Dot Photovoltaics: A Path Forward. *ACS Nano* **2011**, *5*, 8506–8514.
- (32) Kojima, A.; Teshima, K.; Shirai, Y.; Miyasaka, T. Organometal Halide Perovskites as Visible-Light Sensitizers for Photovoltaic Cells. *J. Am. Chem. Soc.* **2009**, *131*, 6050–6051.
- (33) Nozik, A. J.; Memming, R. Physical Chemistry of Semiconductor–Liquid Interfaces. *J. Phys. Chem.* **1996**, *100*, 13061–13078.
- (34) Maldonado, S.; Fitchi, A. G.; Lewis, N. S., Semiconductor/Liquid Junction Photoelectrochemical Solar Cells. In *Series on Photoconversion of Solar Energy. Nanostructured and Photoelectrochemical Systems for Solar Photoconversion*; Archer, M. A., Nozik, A. J., Eds.; Imperial College Press: London, 2010; Vol. 3, pp 537–588.
- (35) Radich, J. G.; Dwyer, R.; Kamat, P. V. Cu<sub>2</sub>S-Reduced Graphene Oxide Composite for High Efficiency Quantum Dot Solar Cells. Overcoming the Redox Limitations of S<sup>2-</sup>/S<sub>n</sub><sup>2-</sup> at the Counter Electrode. *J. Phys. Chem. Lett.* **2011**, *2*, 2453–2460.
- (36) Sudhagar, P.; Jung, J. H.; Park, S.; Lee, Y. G.; Sathyamoorthy, R.; Kang, Y. S.; Ahn, H. The Performance of Coupled (CdS:CdSe) Quantum Dot-Sensitized TiO<sub>2</sub> Nanofibrous Solar Cells. *Electrochem. Commun.* **2009**, *11*, 2220–2224.
- (37) Yu, X.-Y.; Liao, J.-Y.; Qiu, K.-Q.; Kuang, D.-B.; Su, C.-Y. Dynamic Study of Highly Efficient CdS/CdSe Quantum Dot-Sensitized Solar Cells Fabricated by Electrodeposition. *ACS Nano* **2011**, *5*, 9494–9500.
- (38) Gonzalez-Pedro, V.; Xu, X.; Mora-Sero, I.; Bisquert, J. Modeling High-Efficiency Quantum Dot Sensitized Solar Cells. *ACS Nano* **2010**, *4*, 5783–5790.
- (39) Pradhan, N.; Sarma, D. D. Advances in Light-Emitting Doped Semiconductor Nanocrystals. *J. Phys. Chem. Lett.* **2011**, *2*, 2818–2826.
- (40) Santra, P. K.; Kamat, P. V. Mn-Doped Quantum Dot Sensitized Solar Cells. A Strategy to Boost Efficiency over 5%. *J. Am. Chem. Soc.* **2012**, *134*, 2508–2511.
- (41) Bhargava, R. N.; Gallagher, D.; Hong, X.; Nurmikko, A. Optical-Properties of Manganese-Doped Nanocrystals of ZnS. *Phys. Rev. Lett.* **1994**, *72*, 416–419.
- (42) Jana, S.; Srivastava, B. B.; Pradhan, N. Correlation of Dopant States and Host Bandgap in Dual-Doped Semiconductor Nanocrystals. *J. Phys. Chem. Lett.* **2011**, *2*, 1747–1752.
- (43) Beaulac, R.; Archer, P. I.; Ochsenein, S. T.; Gamelin, D. R. Mn<sup>2+</sup>-Doped CdSe Quantum Dots: New Inorganic Materials for Spin-Electronics and Spin-Photonics. *Adv. Funct. Mater.* **2008**, *18*, 3873–3891.
- (44) Beaulac, R.; Archer, P. I.; Gamelin, D. R. Luminescence in Colloidal Mn<sup>2+</sup>-Doped semiconductor Nanocrystals. *J. Solid State Chem.* **2008**, *181*, 1582–1589.
- (45) Zeng, R.; Rutherford, M.; Xie, R.; Zou, B.; Peng, X. Synthesis of Highly Emissive Mn-Doped ZnSe Nanocrystals without Pyrophoric Reagents. *Chem. Mater.* **2010**, *22*, 2107–2113.
- (46) Norris, D. J.; Efros, A. L.; Erwin, S. C. Doped Nanocrystals. *Science* **2008**, *319*, 1776–1779.
- (47) Karan, N. S.; Sarma, D. D.; Kadam, R. M.; Pradhan, N. Doping Transition Metal (Mn or Cu) Ions in Semiconductor Nanocrystals. *J. Phys. Chem. Lett.* **2010**, *1*, 2863–2866.
- (48) Nag, A.; Cherian, R.; Mahadevan, P.; Gopal, A. V.; Hazarika, A.; Mohan, A.; Vengurlekar, A. S.; Sarma, D. D. Size-Dependent Tuning of Mn<sup>2+</sup> d Emission in Mn<sup>2+</sup>-Doped CdS Nanocrystals: Bulk vs Surface. *J. Phys. Chem. C* **2010**, *114*, 18323–18329.
- (49) Beaulac, R.; Archer, P. I.; Liu, X. Y.; Lee, S.; Salley, G. M.; Dobrowolska, M.; Furdyna, J. K.; Gamelin, D. R. Spin-Polarizable Excitonic Luminescence in Colloidal Mn<sup>2+</sup>-Doped CdSe Quantum Dots. *Nano Lett.* **2008**, *8*, 1197–1201.
- (50) Vlaskin, V. A.; Janssen, N.; van Rijssel, J.; Beaulac, R.; Gamelin, D. R. Tunable Dual Emission in Doped Semiconductor Nanocrystals. *Nano Lett.* **2010**, *10*, 3670–3674.
- (51) McDaniel, H.; Fuke, N.; Pietryga, J. M.; Klimov, V. I. Engineered CuInSe<sub>2</sub>S<sub>2-x</sub> Quantum Dots for Sensitized Solar Cells. *J. Phys. Chem. Lett.* **2013**, *4*, 355–361.
- (52) Li, L. A.; Pandey, A.; Werder, D. J.; Khanal, B. P.; Pietryga, J. M.; Klimov, V. I. Efficient Synthesis of Highly Luminescent Copper Indium Sulfide-Based Core/Shell Nanocrystals with Surprisingly Long-Lived Emission. *J. Am. Chem. Soc.* **2011**, *133*, 1176–1179.
- (53) Santra, P. K.; Kamat, P. V. Quantum Dot Solar Cells Research at Notre Dame. In *Frontiers of Quantum Dot Solar Cells*; Toyoda, T., Ed.; CMC Publishing: Tokyo, Japan, 2012; pp 156–161.
- (54) Santra, P. K.; Nair, P. V.; Thomas, K. G.; Kamat, P. V. CuInS<sub>2</sub> Sensitized Quantum Dot Solar Cell. Electrophoretic Deposition, Excited State Dynamics and Photovoltaic Performance. *J. Phys. Chem. Lett.* **2013**, *4*, 722–729.
- (55) Tvrđy, K.; Frantszov, P.; Kamat, P. V. Photoinduced Electron Transfer from Semiconductor Quantum Dots to Metal Oxide Nanoparticles. *Proc. Natl. Acad. Sci. U.S.A.* **2011**, *108*, 29–34.
- (56) Chakrapani, V.; Baker, D.; Kamat, P. V. Understanding the Role of the Sulfide Redox Couple (S<sup>2-</sup>/S<sub>n</sub><sup>2-</sup>) in Quantum Dot Sensitized Solar Cells. *J. Am. Chem. Soc.* **2011**, *133*, 9607–9615.
- (57) Nozik, A. J. Nanoscience and Nanostructures for Photovoltaics and Solar Fuels. *Nano Lett.* **2010**, *10*, 2735–2741.
- (58) Beard, M. C. Multiple Exciton Generation in Semiconductor Quantum Dots. *J. Phys. Chem. Lett.* **2011**, *2*, 1282–1288.
- (59) McGuire, J. A.; Joo, J.; Pietryga, J. M.; Schaller, R. D.; Klimov, V. I. New Aspects of Carrier Multiplication in Semiconductor Nanocrystals. *Acc. Chem. Res.* **2008**, *41*, 1810–1819.
- (60) Tisdale, W. A.; Williams, K. J.; Timp, B. A.; Norris, D. J.; Aydil, E. S.; Zhu, X. Y. Hot-Electron Transfer from Semiconductor Nanocrystals. *Science* **2010**, *328*, 1543–1547.
- (61) Nair, G.; Chang, L.-Y.; Geyer, S. M.; Bawendi, M. G. Perspective on the Prospects of a Carrier Multiplication Nanocrystal Solar Cell. *Nano Lett.* **2011**, *11*, 2145–2151.
- (62) Sambur, J. B.; Novet, T.; Parkinson, B. A. Multiple Exciton Collection in a Sensitized Photovoltaic System. *Science* **2010**, *330*, 63–66.
- (63) Trinh, M. T.; Limpens, R.; de Boer, W. D. A. M.; Schins, J. M.; Siebbeles, L. D. A.; Gregorkiewicz, T. Direct Generation of Multiple Excitons in Adjacent Silicon Nanocrystals Revealed by Induced Absorption. *Nat. Photonics* **2012**, *6*, 316–321.
- (64) Pandey, A.; Guyot-Sionnest, P. Hot Electron Extraction from Colloidal Quantum Dots. *J. Phys. Chem. Lett.* **2010**, *1*, 45–47.
- (65) Miaja-Avila, L.; Tritsch, J. R.; Wolcott, A.; Chan, W. L.; Nelson, C. A.; Zhu, X. Y. Direct Mapping of Hot-Electron Relaxation and Multiplication Dynamics in PbSe Quantum Dots. *Nano Lett.* **2012**, *12*, 1588–1591.
- (66) Kirk, A. P.; Fischetti, M. V. Fundamental Limitations of Hot-Carrier Solar Cells. *Phys. Rev. B* **2012**, *86*, 165206.
- (67) Semonin, O. E.; Luther, J. M.; Choi, S.; Chen, H. Y.; Gao, J. B.; Nozik, A. J.; Beard, M. C. Peak External Photocurrent Quantum Efficiency Exceeding 100% via MEG in a Quantum Dot Solar Cell. *Science* **2011**, *334*, 1530–1533.
- (68) Achermann, M. Exciton-Plasmon Interactions in Metal-Semiconductor Nanostructures. *J. Phys. Chem. Lett.* **2010**, *1*, 2837–2843.
- (69) Standridge, S. D.; Schatz, G. C.; Hupp, J. T. Toward Plasmonic Solar Cells: Protection of Silver Nanoparticles via Atomic Layer Deposition of TiO<sub>2</sub>. *Langmuir* **2009**, *25*, 2596–2600.
- (70) Kulkarni, A. P.; Noone, K. M.; Munechika, K.; Guyer, S. R.; Ginger, D. S. Plasmon-Enhanced Charge Carrier Generation in Organic Photovoltaic Films Using Silver Nanoprisms. *Nano Lett.* **2010**, *10*, 1501–1505.
- (71) Qi, J.; Dang, X.; Hammond, P. T.; Belcher, A. M. Highly Efficient Plasmon-Enhanced Dye-Sensitized Solar Cells through Metal@Oxide Core@Shell Nanostructure. *ACS Nano* **2011**, *5*, 7108–7116.
- (72) Gao, H.; Liu, C.; Jeong, H. E.; Yang, P. Plasmon-Enhanced Photocatalytic Activity of Iron Oxide on Gold Nanopillars. *ACS Nano* **2012**, *6*, 234–240.
- (73) Awazu, K.; Fujimaki, M.; Rockstuhl, C.; Tominaga, J.; Murakami, H.; Ohki, Y.; Yoshida, N.; Watanabe, T. A Plasmonic Photocatalyst Consisting of Silver Nanoparticles Embedded in Titanium Dioxide. *J. Am. Chem. Soc.* **2008**, *130*, 1676–1680.

- (74) Liu, Z.; Hou, W.; Pavaskar, P.; Aykol, M.; Cronin, S. B. Plasmon Resonant Enhancement of Photocatalytic Water Splitting Under Visible Illumination. *Nano Lett.* **2011**, *11*, 1111–1116.
- (75) Hägglund, C.; Apell, S. P. Plasmonic Near-Field Absorbers for Ultrathin Solar Cells. *J. Phys. Chem. Lett.* **2012**, *3*, 1275–1285.
- (76) Warren, S. C.; Walker, D. A.; Grzybowski, B. A. Plasmonics: Coupling Plasmonic Excitation with Electron Flow. *Langmuir* **2012**, *28*, 9093–9102.
- (77) Gomez, D. E.; Vernon, K. C.; Mulvaney, P.; Davis, T. J. Surface Plasmon Mediated Strong Exciton–Photon Coupling in Semiconductor Nanocrystals. *Nano Lett.* **2009**, *10*, 274–278.
- (78) Ma, X.; Fletcher, K.; Kipp, T.; Grzelczak, M. P.; Wang, Z.; Guerrero-Martinez, A.; Pastoriza-Santos, I.; Kornowski, A.; Liz-Marzán, L. M.; Mews, A. Photoluminescence of Individual Au/CdSe Nanocrystal Complexes with Variable Interparticle Distances. *J. Phys. Chem. Lett.* **2011**, *2*, 2466–2471.
- (79) Li, M.; Cushing, S. K.; Wang, Q.; Shi, X.; Hornak, L. A.; Hong, Z.; Wu, N. Size-Dependent Energy Transfer between CdSe/ZnS Quantum Dots and Gold Nanoparticles. *J. Phys. Chem. Lett.* **2011**, *2*, 2125–2129.
- (80) Ferry, V. E.; Munday, J. N.; Atwater, H. A. Design Considerations for Plasmonic Photovoltaics. *Adv. Mater.* **2010**, *22*, 4794–4808.
- (81) Beck, F. J.; de Arquer, F. P. G.; Bernechea, M.; Konstantatos, G. Electrical Effects of Metal Nanoparticles Embedded in Ultra-Thin Colloidal Quantum Dot Films. *Appl. Phys. Lett.* **2012**, *101*, 041103.
- (82) Choi, H.; Chena, W. T.; Kamat, P. V. Know Thy Nano Neighbor. Plasmonic versus Electron Charging Effects of Gold Nanoparticles in Dye Sensitized Solar Cells. *ACS Nano* **2012**, *6*, 4418–4427.
- (83) Hotchandani, S.; Kamat, P. V. Modification of Electrode Surface with Semiconductor Colloids and its Sensitization with Chlorophyll *a*. *Chem. Phys. Lett.* **1992**, *191*, 320–326.
- (84) Mora-Sero, I.; Ditttrich, T.; Susa, A. S.; Rogach, A. L.; Bisquert, J. Large Improvement of Electron Extraction from CdSe Quantum Dots into a TiO<sub>2</sub> Thin Layer by N3 Dye Coabsorption. *Thin Solid Films* **2008**, *516*, 6994–6998.
- (85) Mora-Seró, I.; Gross, D.; Mittereder, T.; Lutich, A. A.; Susa, A. S.; Ditttrich, T.; Belaidi, A.; Caballero, R.; Langa, F.; Bisquert, J.; et al. Nanoscale Interaction Between CdSe or CdTe Nanocrystals and Molecular Dyes Fostering or Hindering Directional Charge Separation. *Small* **2009**, *6*, 221–225.
- (86) Choi, H.; Nicolaescu, R.; Paek, S.; Ko, J.; Kamat, P. V. Supersensitization of CdS Quantum Dots with NIR Organic Dye: Towards the Design of Panchromatic Hybrid-Sensitized Solar Cells. *ACS Nano* **2011**, *5*, 9238–9245.
- (87) Shalom, M.; Albero, J.; Tachan, Z.; Martinez-Ferrero, E.; Zaban, A.; Palomares, E. Quantum Dot–Dye Bilayer-Sensitized Solar Cells: Breaking the Limits Imposed by the Low Absorbance of Dye Monolayers. *J. Phys. Chem. Lett.* **2010**, *1*, 1134–1138.
- (88) Buhbut, S.; Itzhakov, S.; Tauber, E.; aShalom, M.; Hod, I.; Geiger, T.; Garini, Y.; Oron, D.; Zaban, A. Built-in Quantum Dot Antennas in Dye-Sensitized Solar Cells. *ACS Nano* **2010**, *4*, 1293–1298.
- (89) Choi, H.; Santra, P. K.; Kamat, P. V. Synchronized Energy and Electron Transfer Processes in Covalently Linked CdSe–Squaraine Dye–TiO<sub>2</sub> Light Harvesting Assembly. *ACS Nano* **2012**, *6*, 5718–5726.
- (90) Deng, M. H.; Zhang, Q. X.; Huang, S. Q.; Li, D. M.; Luo, Y. H.; Shen, Q.; Toyoda, T.; Meng, Q. B. Low-Cost Flexible Nano-Sulfide/Carbon Composite Counter Electrode for Quantum-Dot-Sensitized Solar Cell. *Nanoscale Res. Lett.* **2010**, *5*, 986–990.
- (91) Tian, J.; Gao, R.; Zhang, Q.; Zhang, S.; Li, Y.; Lan, J.; Qu, X.; Cao, G. Enhanced Performance of CdS/CdSe Quantum Dot Cosensitized Solar Cells via Homogeneous Distribution of Quantum Dots in TiO<sub>2</sub> Film. *J. Phys. Chem. C* **2012**, *116*, 18655–18662.
- (92) Shalom, M.; Buhbut, S.; Tirosh, S.; Zaban, A. Design Rules for High-Efficiency Quantum-Dot-Sensitized Solar Cells: A Multilayer Approach. *J. Phys. Chem. Lett.* **2012**, *3*, 2436–2441.
- (93) Leschkie, K. S.; Divakar, R.; Basu, J.; Enache-Pommer, E.; Boercker, J. E.; Carter, C. B.; Kortshagen, U. R.; Norris, D. J.; Aydil, E. S. Photosensitization of ZnO Nanowires with CdSe Quantum Dots for Photovoltaic Devices. *Nano Lett.* **2007**, *7*, 1793–1798.
- (94) Tena-Zaera, R.; Katty, A.; Bastide, S.; Levy-Clement, C. Annealing Effects on the Physical Properties of Electrodeposited ZnO/CdSe Core–Shell Nanowire Arrays. *Chem. Mater.* **2007**, *19*, 1626–1632.
- (95) Tak, Y.; Hong, S. J.; Lee, J. S.; Yong, K. Fabrication of ZnO/CdS Core/Shell Nanowire Arrays for Efficient Solar Energy Conversion. *J. Mater. Chem.* **2009**, *19*, 5945–5951.
- (96) Wallentin, J.; Anttu, N.; Asoli, D.; Huffman, M.; Åberg, I.; Magnusson, M. H.; Siefert, G.; Fuss-Kailuweit, P.; Dimroth, F.; Witzigmann, B. InP Nanowire Array Solar Cells Achieving 13.8% Efficiency by Exceeding the Ray Optics Limit. *Science* **2013**, *339*, 1057–1060.
- (97) Huynh, W. U.; Dittmer, J. J.; Alivisatos, A. P. Hybrid Nanorod–Polymer Solar Cells. *Science* **2002**, *295*, 2425–2427.
- (98) Gur, I.; Fromer, N. A.; Geier, M. L.; Alivisatos, A. P. Air-Stable All-Inorganic Nanocrystal Solar Cells Processed from Solution. *Science* **2005**, *310*, 462–464.
- (99) Yu, Y.; Kamat, P. V.; Kuno, M. A CdSe Nanowire/Quantum Dot Hybrid Architecture for Improving Solar Cell Performance. *Adv. Funct. Mater.* **2010**, *20*, 1464–1472.
- (100) Lightcap, I. V.; Kamat, P. V. Fortification of CdSe Quantum Dots with Graphene Oxide. Excited State Interactions and Light Energy Conversion. *J. Am. Chem. Soc.* **2012**, *134*, 7109–7116.
- (101) Lightcap, I. V.; Kamat, P. V. Graphitic Design: Prospects of Graphene-Based Nanocomposites for Solar Energy Conversion, Storage, and Sensing. *Acc. Chem. Res.* **2013**, DOI: 10.1021/ar300248f.
- (102) Farrow, B.; Kamat, P. V. CdSe Quantum Dot Sensitized Solar Cells. Shuttling Electrons through Stacked Carbon Nanocups. *J. Am. Chem. Soc.* **2009**, *131*, 11124–11131.
- (103) Lightcap, I. V.; Murphy, S.; Schumer, T.; Kamat, P. V. Electron Hopping Through Single-to-Few Layer Graphene Oxide Films. Photocatalytically Activated Metal Nanoparticle Deposition. *J. Phys. Chem. Lett.* **2012**, *3*, 1453–1458.
- (104) Genovese, M. P.; Lightcap, I. V.; Kamat, P. V. Sun-Believable Solar Paint. A Transformative One-Step Approach for Designing Nanocrystalline Solar Cells. *ACS Nano* **2012**, *6*, 865–872.
- (105) Panthani, M. G.; Akhavan, V.; Goodfellow, B.; Schmidtke, J. P.; Dunn, L.; Dodabalapur, A.; Barbara, P. F.; Korgel, B. A. Synthesis of CuInS<sub>2</sub>, CuInSe<sub>2</sub>, and Cu(In<sub>x</sub>Ga<sub>1-x</sub>)Se<sub>2</sub> (CIGS) Nanocrystal “Inks” for Printable Photovoltaics. *J. Am. Chem. Soc.* **2008**, *130*, 16770–16777.